Introduction

Hepatocellular carcinoma (HCC) is one of the most common types of malignant tumors worldwide. It is the fifth leading cause of cancer death, and is associated with a relatively low prevalence of survival at 5 years [1]. Systemic chemotherapies have been thought to be the most promising strategies for patients with HCC [2–4]. However, many of these conventional chemotherapies have not been shown to improve survival, primarily because HCC is highly resistant against such chemotherapies [2–4]. In addition, many conventional anti-tumor agents do not selectively kill HCC cells, which can lead to undesirable side effects [3]. Many researchers have therefore attempted to develop tumor-selective carriers (e.g., polymers, liposomes, proteins) for drug delivery systems (DDS) based mainly on active targeting strategies (e.g., folic acid, peptide ligands, and antibody-modification with carriers) [5–7].

Recently, a short peptide ligand termed SP94 (SFSIIHTPILPL) was discovered using an *in-vivo* phase display technique, and was shown to bind selectively to various types of HCC cells [8]. Moreover, SP94-displayed liposome-containing chemotherapeutic agents exhibit much higher affinity toward various types of HCC cells compared with normal cells (including normal hepatocytes, endothelial cells, and immune cells) and killed HCC cells [9]. Thus, SP94 peptide could be useful as a HCC cell-targeted ligand and could be available for developing HCC-targeted DDS. In general, compared with antibodies, peptide ligands have advantages such as easier synthesis, lower expense, and lower immunogenesis. However, the effects of peptide conjugation methodologies (e.g., peptide content; site of peptide conjugation; effect of linker length between peptides and carriers on affinity of engineered carriers toward HCC cells) have not been thoroughly investigated, even though these factors will be very important for the development of effective drug carriers.

In this study, we described a human HCC-targeted nanoparticle which was chemically modified SP94 peptides at the exterior of the nanoparticle (**Figure 1A**). As a model nanoparticle, we focused on small heat shock protein 16.5 (Hsp), a naturally occurring protein in *Methanococcus jannaschii*, which forms a "cage" structure through self-assembly of 24 subunit proteins (i.e. outer size and inner size are 12 nm and 6.5 nm, respectively) (**Figure 1A**) [10]. Hsp is attractive as a biomedical tool for delivery of therapeutics, imaging device, and sensing material due to its biocompatibility, monodispersed formation, robust structure, easy acquisition from *Escherichia coli*, and easy functionalization through chemical and genetic strategies [11–20]. However, Hsp does not have sufficient specificity for cells or tissues, which is a major obstacle to its application as a drug carrier or imaging device. Therefore, providing specificity towards certain cells or tissues for Hsp is very important for disease treatment and diagnostic imaging.

We first synthesized six types of engineered "protein cages" which were different in (i) SP94 peptide contents, (ii) conjugation site of SP94 peptide and (iii) linker length between an Hsp cage and an SP94 peptide. Synthesized Hsp cage–SP94 peptide conjugates were analyzed using matrix-assisted laser desorption/ionization-time of flight mass spectrometry (MALDI-ToF MS) analyses, sodium dodecyl sulfate-polyacrylamide gel electrophoresis (SDS-PAGE) analyses and dynamic light scattering (DLS) measurement. Observation of fluorescence microscopic images revealed all of the engineered Hsp cages to bind selectively to human HCC cells (HepG2 and Huh-7 cells) but not to other cell lines, including human cervical carcinoma (HeLa) cells and rat normal hepatocytes (RLN-8). Interestingly, the level of binding of HCC cells of engineered protein cages was changed appreciably according to: (i) peptide content, (ii) conjugation site of peptides and (iii) linker length. These results provide useful information to enhance cellular uptake of peptide ligand-fabricated nanoparticles by changing the chemical conjugation strategy of peptide ligands.

Materials and methods

Expression and purification of HspG41C cages

The pET21a(+) vector-encoded HspG41C mutant in which the Gly residue at position 41 of wild-type Hsp was substituted with a Cys residue was prepared by polymerase chain reaction (PCR)-mediated mutagenesis using the appropriate primers. The success of mutagenesis was confirmed by DNA sequencing. HspG41C mutant protein was expressed from *E. coli*, and was purified using anion exchange

chromatography and size-exclusion chromatography (SEC). BL21 Gold (DE3) (Novagene, Tokyo, Japan) was used as a strain for HspG41C.

E. coli containing the pET21a(+) plasmid vector were grown in 2×YT medium containing 100 μg/mL of ampicillin at 37°C. When the optical density (OD) at 600 nm of the culture medium reached between 0.5 and 0.6, expression of a recombinant protein was induced with 1 mM of isopropyl-β-$_D$-thiogalactopyranoside (IPTG) (Wako Pure Chemical Ind. Ltd., Osaka, Japan) for 4 h at 37°C. After collection of cells by centrifugation, cells were suspended in 25 mM KH_2PO_4 solution (containing 1 mM ethylenediamine tetra-acetic acid (EDTA) and 2 mM dithiothreitol (DTT), pH 7.0) and stored at –80°C until purification. Cell suspensions were sonicated to disrupt the cell membrane. Cell lysate solutions were then centrifuged at 15,000 rpm for 30 min at 4°C and then supernant collected. Proteins were purified using a HiLoad 26/10 QSepharose HP anion exchange column (GE Healthcare, Buckinghamshire, UK) and a SEC column (TSK gel G3000SW; Tosoh, Tokyo, Japan). Purification was confirmed by 15% SDS-PAGE analyses.

Synthesis of Alexa488-modified HspG41C (HspG41C-Alx)

For modification of fluorophores on the interior of HspG41C, HspG41C (2.5 mg, 152 nmol Cys residues) was reacted with Alexa-Fluor® 488 C_5-maleimide (0.13 mg, 182 nmol) (Invitrogen, Carlsbad, CA, USA) in 0.1 M phosphate buffer (PB; pH 7.2) for 2 h at room temperature. The reactant was further incubated for 20 h at 4°C. Unreacted Alexa-Fluor® 488 C_5-maleimide was removed by ultrafiltration using Amicon Ultra Centrifugal Filters with MWCO 100,000 (Millipore, Tokyo, Japan). The success of Alexa488 modification to HspG41C was confirmed using MALDI-ToF MS analyses.

Synthesis of SP94 peptide-modified HspG41C-Alx

To introduce maleimide groups to Hsp cages, hetero-bifunctional polyethylene glycol linkers possessing succinimidyl and maleimide groups at the end of linkers (SM(PEG)$_n$; n = 12 or 24; Thermo Scientific, Kanagawa, Japan) were used. HspG41C-Alx was modified with SM(PEG)$_n$ (50-times excess of the protein monomer) through amide bonds in PB (0.1 M, pH 7.2) for 2 h at room temperature, followed by removal of unreacted SM(PEG)$_n$ by ultrafiltration as described above to obtain HspG41C-Alx-SM(PEG)$_n$-containing maleimide groups.

For modification of SP94 peptide, two types of SP94 peptides containing a Cys residue at the *N*-terminus or *C*-terminus were prepared; sequences of peptide *1* and *2* were Ac-CGGSFSIIHTPILPL-NH_2 and Ac-SFSIIHTPILPLGGC-NH_2, respectively (the underline indicates the SP94 peptide sequence). HspG41C-Alx-SM(PEG)$_n$ and SP94 peptides (2 eq. or 10 eq. to protein monomer) were dissolved in PB (0.1 M, pH 7.2) and stirred for 6 h at room temperature, and allowed to stand for 20 h at 4°C. The mixture was purified by ultrafiltration as described above.

MALDI-ToF MS analyses

Measurement of the molecular weight of PEG-modified HspG41C cages was undertaken by MALDI-ToF MS analyses using Autoflex Speed (Bruker Daltonics Inc., Billerica, MA, USA). Sinapinic acid (Bruker Daltonic Inc.) was used as a matrix.

SDS-PAGE analyses

SDS-PAGE was undertaken using 15% SDS-PAGE gel (Wako Pure Chemical. Ind.). Sample bands were imaged by the fluorescence of Alexa488 bound to each protein cage using a Typhoon FLA9000 Biomolecular Imager (GE Healthcare). Fluorescence images were analyzed using ImageQuant TL (GE Healthcare).

Measurement of the size of SP94-modified HspG41C cages by DLS

All samples and buffer solutions were filtered using Ultrafree-MC with pore sizes of 0.22 μm (Millipore, Tokyo, Japan) before DLS measurement. Sizes of protein cages (0.1 mg/mL) were measured thrice using a Zetasizer Nano ZS Analyzer (Malvern, UK) at 25°C.

Cell culture

Human HCC (Huh-7 and HepG2), human cervical carcinoma HeLa, and rat normal liver cell RLN-8 cells were cultured in the appropriate medium containing 10% fetal bovine serum (FBS), 100 U/mL penicillin, 100 μg/mL streptomycin, and 0.25 μg/mL amphotericin-B (all from Gibco, NY, USA) in a humidified atmosphere of 5% CO_2 and 95% air at 37°C. Dulbecco's modified Eagle's medium (DMEM) was used for cultivation of Huh-7 and HepG2 cells, Eagle's minimal essential medium (EMEM) containing non-essential amino acids for HeLa cells, and minimal essential medium α (MEMα) for RLN-8 cells (all from Wako) were used.

Fluorescence microscopic observation

Cells were seeded on 96-well culture plates with an initial cell density of 10,000/well and cultured for 1 day in 100 μL of the appropriate medium containing 10% FBS. Final concentrations of Hsp cages were adjusted to 40 nM (1 μM of subunit protein) by Opti-MEM (Gibco) and 100 μL of diluted Hsp cages was added to each well. After incubation for 24 h, the medium was changed to fresh Opti-MEM containing 5 μg/mL of Hoechst 33342 (Dojindo, Kumamoto, Japan), and incubated for 1 h. Fluorescence images were obtained using fluorescence microscope BZ-9000 (Keyence, Osaka, Japan).

Fluorescence measurement of cellular uptake of HspG41C-SM(PEG)$_n$–SP94 peptide conjugates

Huh-7 and HepG2 cells were harvested on 96-well plates with an initial cell density of 10,000/well, and cultured for 1 day. Fifty-microliters of each protein cage diluted with Opti-MEM (4 nM) were added to each well. After incubation for 24 h, cells were rinsed twice with phosphate-buffered saline (PBS)(–) and then lysed in 100 μL of buffer (pH 7.5, 20 mM Tris-HCl, 2 mM EDTA, and 0.05% Triton-X 100). Lysate solutions were replaced on black-bottomed 96 well-plates and the fluorescence intensity of each sample measured using a Microplate Reader (ARVO MX 1420; Perkin Elmer Inc., Waltham, MA, USA).

Results and discussion

Synthesis and characterization of HCC-targeted peptide- and fluorophore-modified HspG41C cages

The synthetic scheme of HspG41C-Alx-SP94 is described in **Figure 1(B)**. HspG41C was labeled with Alexa488-maleimide at the interior of HspG41C cages *via* thioether bonds between a unique Cys residue of HspG41C and a maleimide group of Alexa488 (HspG41C-Alx). Twenty-one molecules of Alexa488 were modified with each HspG41C-Alx cage (0.88 molecules/monomer protein), which was estimated from the result of MALDI-ToF MS analyses (**Figure 2A**).

To introduce the maleimide groups into HspG41C-Alx, hetero-bifunctional linkers (SM(PEG)$_{12}$ or SM(PEG)$_{24}$) that possessed NHS ester and maleimide groups at either side of the linkers were conjugated to HspG41C-Alx thorough amide bonds to obtain HspG41C-Alx-SM(PEG)$_n$. MALDI-ToF MS analyses showed that 1–3 molecules of the linker were bound to HspG41C-Alx-SM(PEG)$_n$ (**Figures 2B and C**). Moreover, these corresponding bands were observed from SDS-PAGE analyses (**Figure 3**). SDS-PAGE analyses revealed that, on average, 23 ± 2 molecules of SM(PEG)$_{12}$ and 23 ± 3 molecules of SM(PEG)$_{24}$ were bound to HspG41C-Alx-SM(PEG)$_{12}$ and HspG41C-Alx-SM(PEG)$_{24}$, respectively (**Figure 3**).

To conjugate SP94 peptides into HspG41C-Alx-SM(PEG)$_n$, two SP94 peptide derivatives containing a Cys residue at the *N*-terminus or *C*-terminus of the original SP94 peptide sequences were prepared; i.e. peptide *1* and peptide *2* possessed a Cys residue at the *N*-terminus and *C*-terminus of the original SP94 peptide sequences, respectively. Peptide *1* or *2* was modified with HspG41C-Alx-SM(PEG)$_n$ through a Michael addition reaction between a thiol group of a SP94 peptide derivative and maleimide groups of HspG41C-Alx-SM(PEG)$_n$. SDS-PAGE analyses revealed that peptide *1* and *2* were successfully modified with HspG41C-Alx-SM(PEG)$_{12}$ because three new bands corresponding to HspG41C-Alx-SM(PEG)$_{12}$ bound to one or two SP94 peptide molecules per protein monomer were observed (lanes 3–6) (**Figure 3A**). Moreover, one SP94 peptide per protein monomer could conjugate into HspG41C-Alx-SM(PEG)$_{24}$ (**Figure 3B**). Average SP94 peptide contents in each

HspG41C-Alx-SM(PEG)$_n$ were determined from SDS-PAGE analyses (**Figure 3**) and are summarized in **Table 1**.

Size measurements of linker- and peptide-modified HspG41C

Sizes of HspG41C conjugates in PBS were measured by DLS analyses. HspG41C is known to form a cage structure with a diameter of 12 nm [10]. The HspG41C used in the present study also showed a comparable size (**Figure 4A**). After conjugation of SM(PEG)$_n$ linkers to HspG41C, a slightly larger size from HspG41C-SM(PEG)$_n$ was observed compared with that from HspG41C. Moreover, HspG41C-SM(PEG)$_{24}$ showed a larger size than HspG41C-SM(PEG)$_{12}$ due to a longer length of SM(PEG)$_{24}$ compared with SM(PEG)$_{12}$ (i.e., the lengths of SM(PEG)$_{24}$ and SM(PEG)$_{12}$ were 9.5 nm and 5.3 nm, respectively). In addition, HspG41C-SM(PEG)$_n$ did not form large aggregates (>100 nm) (**Figure 4A, inset**).

All of the HspG41C-SM(PEG)$_{12}$–SP94 peptide conjugates showed slightly larger sizes than HspG41C-SM(PEG)$_{12}$, and the sizes of HspG41C-SM(PEG)$_{12}$–P94 peptide conjugates were changed depending on peptide contents (**Figure 4B**). Furthermore, identical trends were observed from the system of HspG41C-SM(PEG)$_{24}$–SP94 peptide conjugates (**Figure 4C**). All of the HspG41C-SM(PEG)$_n$–SP94 peptide conjugates showed formation of large aggregate (>100 nm) (**Figures 4B and C, inset**). These results showed that the cage structure of HspG41C was sufficiently robust for chemical modification of target peptides.

Fluorescence microscopic observation of cellular binding of HspG41C-SM(PEG)$_n$–SP94 peptide conjugates toward various types of cell lines

To verify if HspG41C-SM(PEG)$_n$–SP94 peptide conjugates could bind selectively to HCC cells, Alexa488-labeled conjugates were added to human HCC cell lines (Huh-7 and HepG2), HeLa and RLN-8, and binding of conjugates to cells was then detected using a fluorescence microscope. When Alexa488-labeled HspG41C-SM(PEG)$_n$–SP94 peptide conjugates were added to Huh-7 and HepG2 cells, green fluorescence was observed, indicating that all conjugates could bind human HCC-derived cell lines (**Figure 5A**). However, of the number of protein cages bound to HCC cells changed appreciably according to: (i) SP94 peptide content, (ii) conjugation site of the SP94 peptide, and (3) linker length. In contrast to HCC-derived cells, obvious green fluorescence was not detected after addition of Alexa488-labeled HspG41C-SM(PEG)$_n$–SP94 peptide conjugates to the other cell lines (HeLa and RLN-8 cells). These results showed that HspG41C-SM(PEG)$_n$–SP94 peptide conjugates could bind selectively to human HCC-derived cell lines.

Influence of SP94 peptide content in HspG41C-SM(PEG)$_n$–SP94 peptide conjugates upon cellular binding

To clarify whether SP94 peptide content in HspG41C-SM(PEG)$_n$–SP94 peptide conjugates affected cellular binding, the fluorescence intensity of cellular lysates was compared 24 h after the addition of Alexa-labeled conjugates to HepG2 and Huh-7cells. When 12-N(2) (23 peptides/cage) and 12-N(1) (12 peptides/cage), both of which were modified SP94 peptides at the *N*-terminus of SP94 peptides, were added to HepG2 cells, 12-N(2) showed 3.9-times higher fluorescence intensity than 12-N(1) (**Figure 5B**). Moreover, 2.7-times higher fluorescence intensity from 12-C(2) (22 peptides/cage) was observed when compared with that from 12-C(1) (13 peptides/cage) (**Figure 5B**). Similarly, an increase in SP94 peptide content in conjugates increased the fluorescence intensity in Huh-7 cells, but their variances (≈1.5-times higher) in Huh-7 cells were slightly lower than those in HepG2 cells (**Figure 5C**). Similarly, one study reported that SP94 peptide-displayed liposomes increased their binding to HCC cells with increasing SP94 peptide numbers on liposomes [9]. Therefore, we concluded that an increase in SP94 peptide levels in conjugates could increase the binding of conjugates towards HCC cells due to the multivalent interaction of conjugates.

Influence of SP94 peptide conjugation site (N- or C-terminus) in conjugates upon cellular binding

One study suggested that the *C*-terminal region of SP94 peptide is essential for the binding of HCC cells (SFSIIHTPILPL; consensus sequence shown in the underlined segment) [8]. Thus, we investigated whether the SP94 peptide conjugation site on protein cages (i.e., *N*- or *C*-terminal of SP94 peptide) could affect the affinity of SP94-modified cages toward HCC cells using each conjugate which had identical peptide content and linker length, but different SP94 peptide conjugation site. Protein cages modified by the *N*-terminal of SP94 peptide (12-N(1), 12-N(2) and 24-N(1)) showed 2–11-times higher fluorescence intensity in HepG2 cells compared with those on the *C*-terminal of SP94 peptide (12-C(1), 12-C(2) and 24-C(1)) (i.e., 2.1-times for 12-N(1) *vs* 12-C(1), 2.9 times for 12-N(2) *vs* 12-C(2), and 11 times for 24-N(1) *vs* 24-C(1)) (**Figure 5B**). Similar results were observed in Huh-7 cells (**Figure 5C**). These results strongly suggested that, with respect to cell binding, the SP94 peptide bound to a protein cage at the *N*-terminus of peptides was superior to that at the *C*-terminus of peptides because the *C*-terminal region of SP94 peptide is indispensable to its binding to HCC cells.

Influence of linker length between protein cage and SP94 peptide upon cellular binding

To investigate the effect of linker length between cages and SP94 peptides upon the affinity of engineered cages against HCC cells, the fluorescence intensity of HCC cells was measured after addition of 12-N(1) and 24-N(1) with different numbers of SP94 peptide to HCC cells. The 24-N(1) containing longer linkers showed 4.3-times higher fluorescence intensity than 12-N(1) in HepG2 cells (**Figure 5B**). Similarly, a 2.7-times higher fluorescence intensity in Huh-7 cells was detected from 24-N(1) compared with 12-N(1) (**Figure 5C**). These results suggested that a SP94-modified cage through a longer linker was superior in binding to HCC cells because a longer linker is more flexible, which can make binding of cages to cells easier. Interestingly, 12-C(1) and 24-C(1) exhibited almost comparable fluorescence intensity after their addition into HCC cells. This observation suggested that linker length affected the affinity of cages towards HCC cells only if SP94 peptide was modified with protein cages at the *N*-terminus.

Conclusion

We synthesized an SP94 peptide-modified protein cage (HspG41C-SM(PEG)$_n$-SP94) that could bind selectively to HCC-derived cell lines. An increase in SP94 peptide contents in engineered cages elevated the affinity of cages to HCC cells (especially HepG2 cells). In addition, protein cages modified by the *N*-terminus of SP94 peptides showed higher cellular uptake than those modified by the *C*-terminus. Moreover, an increase in linker length between protein cages and SP94 peptide increased the affinity of conjugates to HCC cells. Collectively, a protein cage modified by the *N*-terminus of SP94 peptide through a longer linker molecule and containing high SP94 peptide levels showed the most effective binding towards HCC cells. These observations could be helpful for developing DDS carriers and imaging systems based on the targeting of peptide ligands. Furthermore, an SP94 peptide-modified Hsp cage is an effective DDS carrier and imaging device towards HCC cells.

Acknowledgments

This work was supported financially by a Grant-in-Aid for Scientific Research from the Ministry of Education, Culture, Sports, Science and Technology (MEXT) of Japan, and Grant-in-Aid for Research Activity Start-up from the MEXT of Japan.

Conflicts of interest

The authors confirm that they have no conflicts of interest.

References

[1] Siegel R, Ward E, Brawley O, Jemal A: **Cancer Statics, 2011: the impact of eliminating socioeconomic and radical disparities on premature cancer deaths.** *CA Cancer J Clin* 2011, **61**:212-236.

[2] Llovet JM, Bruix J: **Molecular targeted therapies in hepatocellular carcinoma.** *Hepatology* 2008, **48**:1312-1327.

[3] Thomas M: **Molecular targeted therapy for hepatocellular carcinoma.** *J Gastroenterol* 2009, **44**: 136-141.

[4] Finn RS: **Development of molecularly targeted therapies in hepatocellular carcinoma: where do we go now?** *Clin Cancer Res* 2010, **16**: 390-397.

[5] Byrne JD, Betancourt T, Brannon-Peppas L: **Active targeting schemes for nanoparticle systems in cancer therapeutics.** *Adv Drug Deliv Rev* 2008, **60**: 1615-1626.

[6] Shimoda A, Sawada S, Akiyoshi K: **Cell specific peptide conjugated polysaccharide nanogels for protein delivery.** *Macromol Biosci* 2011, **11**: 882-888.

[7] Allen TM: **Ligand-targeted therapeutics in anticancer therapy.** *Nat Rev Cancer* 2002, **2**: 750-763.

[8] Lo A, Lin CT, Wu HC: **Hepatocellular carcinoma cell-specific peptide ligand for targeted drug delivery.** *Mol Cancer Ther* 2008, **7**: 579-589.

[9] Ashley CE, Carnes EC, Phillips GK, Padilla D, Durfee PN, Brown PA, Hanna TN, Liu J, Phillips B, Carter MB, Carroll NJ, Jiang X, Dunphy DR, William CL, Petsev DN, Evans DG, Parikh AN, Chackerian B, Wharton W, Peabody DS, Brinker CJ: **The targeted delivery of multicomponent cargos to cancer cells by nanoporous particles-supported lipid bilayers.** *Nat Mater* 2011, **10**: 389-397.

[10] Kim KK, Kim R, Kim SH: **Crystal structure of a small heat-shock protein.** *Nature* 1998, **394**: 595-599.

[11] Flenniken ML, Liepold LO, Crowley BE, Willits DA, Young MJ, Douglas T: **Selective attachment and release of a chemotherapeutic agent from the interior of a protein cage architecture.** *Chem Commun* 2005, 447-449.

[12] Varpness Z, Suci PA, Ensign D, Young MJ, Douglas T: **Photosensitizer efficiency in genetically modified protein cage architectures.** *Chem Commun* 2009, 3726-3728.

[13] Liepold LO, Abedin MJ, Buckhouse ED, Frank JA, Young MJ, Douglas T: **Supramolecular protein cage composite MR contrast agents with extremely efficient relaxivity properties.** *Nano Lett* 2009, **9**: 4520-4526.

[14] Uchida M, Kosuge H, Terashima M, Willits DA, Liepold LO, Young MJ, McConnell MV, Douglas T: **Protein cage nanoparticles bearing the LyP-1 peptide for enhanced imaging of macrophage-rich vascular lesions.** *ACS Nano* 2011, **5**: 2493-2502.

[15] Choi SH, Kwon IC, Hwang KY, Kim IS, Ahn HJ: **Small heat shock protein as a multifunctional scaffold: integrated tumor targeting and caspase imaging within a single cage.** *Biomacromolecules* 2011, **12**: 3099-3106.

[16] Sao K, Murata M, Umezaki K, Fujisaki Y, Mori T, Niidome T, Katayama Y, Hashizume M: **Molecular design of protein-based nanocapsules for stimulus-responsive characteristics.** *Bioorg Med Chem* 2009, **17**: 85-93.

[17] Sao K, Murata M, Fujisaki Y, Umezaki K, Mori T, Niidome T, Katayama Y, Hashizume M: **A novel protease activity assay using a protease-responsive chaperone protein.** *Biochem Biophys Res Commun* 2009, **383**: 293-297.

[18] Flenniken ML, Willits DA, Brumfield S, Young MJ, Douglas T: **The small heat shock protein cage from *Methanococcus jannaschii* is a versatile nanoscale platform for genetic and chemical modification.** *Nano Lett* 2003, **3**: 1573-1576.

[19] Flenniken ML, Willits DA, Harmsen AL, Liepold LO, Harmsen AG, Young MJ, Douglas T: **Melanoma and lymphocyte cell-specific targeting incorporated into a heat shock protein cage architecture.** *Chem Biol* 2006, **13**: 161-170.

[20] Flenniken ML, Uchida M, Liepold LO, Kang S, Young MJ, Douglas T: **A library of protein cage architectures as nanomaterials.** *Curr Top Microbiol Immunol* 2009, **327**: 71-93.

Table 1. Characterization of HspG41C–SP94 peptide conjugates used in this study.

Sample	Peptide number/cage [a]	Conjugated peptide [b]
12-N(1) [c]	12 ± 2	*1*
12-N(2) [c]	23 ± 2	*1*
12-C(1) [c]	13 ± 2	*2*
12-C(2) [c]	22 ± 3	*2*
24-N(1) [d]	15 ± 2	*1*
24-C(1) [d]	16 ± 1	*2*

[a]SP94 peptide contents of each cage were calculated from the results of SDS-PAGE analyses. Data are means ± S.D. of three independent experiments.
[b]Sequences of peptide *1* and *2* were Ac-CGGSFSIIHTPILPL-NH_2 and Ac-SFSIIHTPILPLGGC-NH_2, respectively.
HspG41C–SP94 peptide conjugates were synthesized using [c]HspG41C-Alx-SM$(PEG)_{12}$ or [d]HspG41C-Alx-SM$(PEG)_{24}$ as the precursors.

Figure legends

Figure 1. (A) A SP94-modified Hsp cage (schematic). A Hsp cage consisted of 24 protein subunits with a molecular weight of 16.5 kDa, and formed a hollow-shaped structure. (B) Synthetic scheme of HspG41C–SP94 peptide conjugates.

Figure 2. MALDI-ToF MS analyses of (A) HspG41C-Alx, (B) HspG41C-Alx-SM$(PEG)_{12}$ and (C) HspG41C-Alx-SM$(PEG)_{24}$. Open circles and filled squares indicate HspG41C- and HspG41C-derived peaks, respectively. Theoretical molecular weight of HspG41C and HspG41C-Alx were 16498 g/mol and 17219 g/mol, respectively. Net mass addition through conjugation of one SM$(PEG)_{12}$ and one SM$(PEG)_{24}$ molecule with protein cages were 750 g/mol and 1279 g/mol, respectively.

Figure 3. SDS-PAGE analyses of HspG41C-SP94-peptide conjugates. (A) HspG41C-Alx-SM$(PEG)_{12}$–SP94 peptide conjugates. Lane 1, HspG41C-Alx; lane 2, HspG41C-Alx-SM$(PEG)_{12}$; lane 3, 12-N(1); lane 4, 12-N(2); lane 5, 12-C(1); and lane 6, 12-C(2). (B) HspG41C-Alx-SM$(PEG)_{24}$–SP94 peptide conjugates. Lane 1, HspG41C-Alx-SM$(PEG)_{24}$; lane 2, 24-N(1); and lane 3: 24-C(1). Each band was imaged by fluorescence from Alexa488 conjugated with protein cages. 'L' and 'pep' indicate SM$(PEG)_n$ linker and SP94 peptide, respectively.

Figure 4. Size distributions of (A) HspG41C-SM$(PEG)_n$, (B) HspG41C-SM$(PEG)_{12}$–SP94 peptide conjugates, and (C) HspG41C-SM$(PEG)_{24}$–SP94 peptide conjugates determined by DLS. Measurements were unertaken at least twice, and the results showed almost identical size distributions.

Figure 5. (A) Fluorescence microscopic observation of the uptake of each HspG41C-SM$(PEG)_n$-SP94. Images were obtained 24 h after addition of 40 nM of HspG41C-SM$(PEG)_n$-SP94. Green (Alexa488) and blue (Hoechst33342) colors indicate HspG41C-SM$(PEG)_n$-SP94 and the nucleus, respectively. Experiments were undertaken at least thrice. Fluorescence intensity in (B) HepG2 and (C) Huh-7 cells after addition of each HspG41C-SM$(PEG)_n$-SP94. Twenty-four hours after the addition of 4 nM of protein cages, cells were lysed in lysis buffer (20 mM Tris-HCl, 2 mM EDTA, and 0.05% Triton-X 100 at pH 7.4), and the fluorescence intensity of lysate solution measured using a microplate reader. Data are means ± S.D. of three independent experiments.

Figure 1.

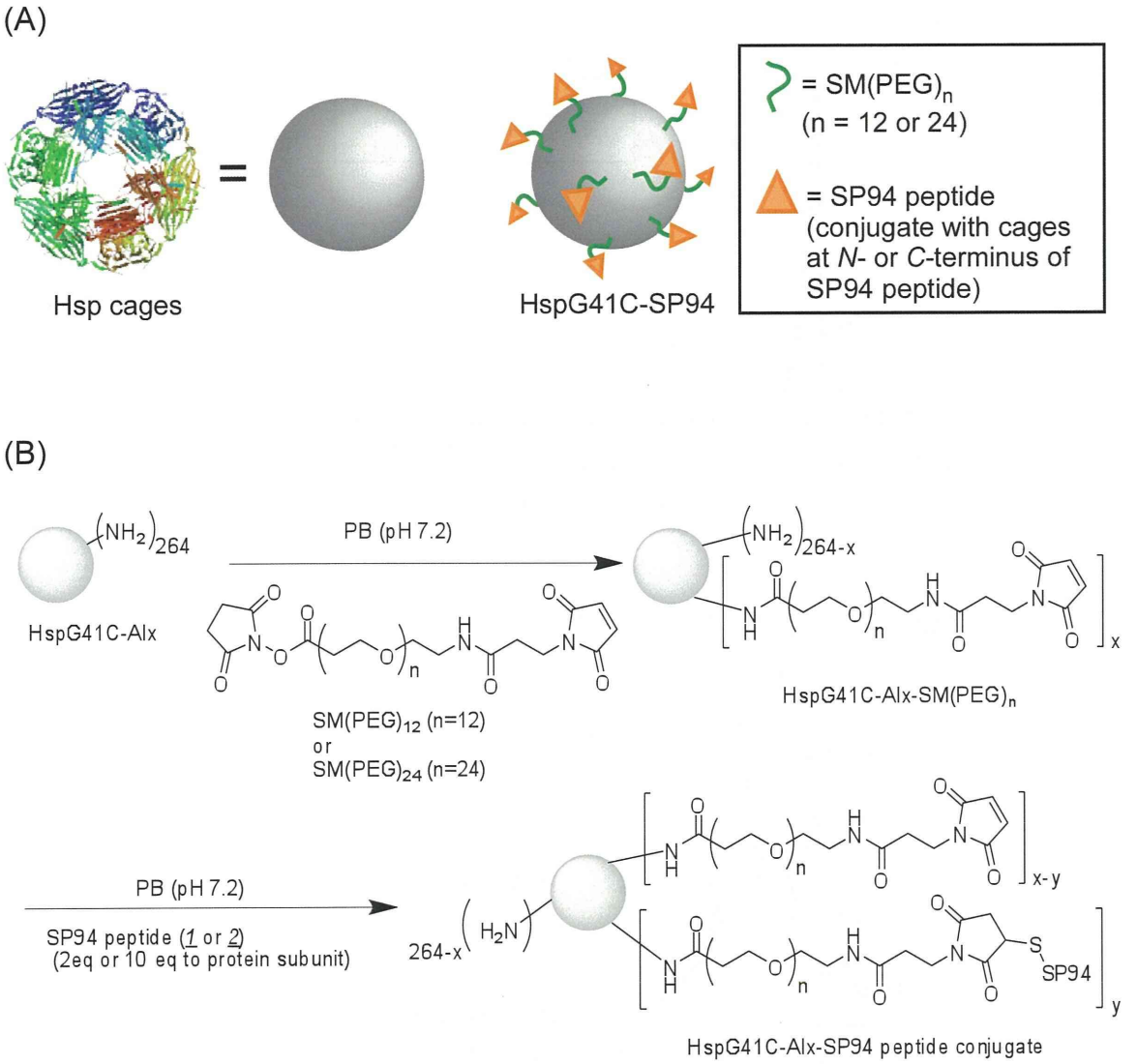
(A)
Hsp cages
HspG41C-SP94
= SM(PEG)n
(n = 12 or 24)
= SP94 peptide
(conjugate with cages
at N- or C-terminus of
SP94 peptide)
(B)
HspG41C-Alx
PB (pH 7.2)
SM(PEG)12 (n=12)
or
SM(PEG)24 (n=24)
HspG41C-Alx-SM(PEG)n
PB (pH 7.2)
SP94 peptide (1 or 2)
(2eq or 10 eq to protein subunit)
HspG41C-Alx-SP94 peptide conjugate

Figure 2.

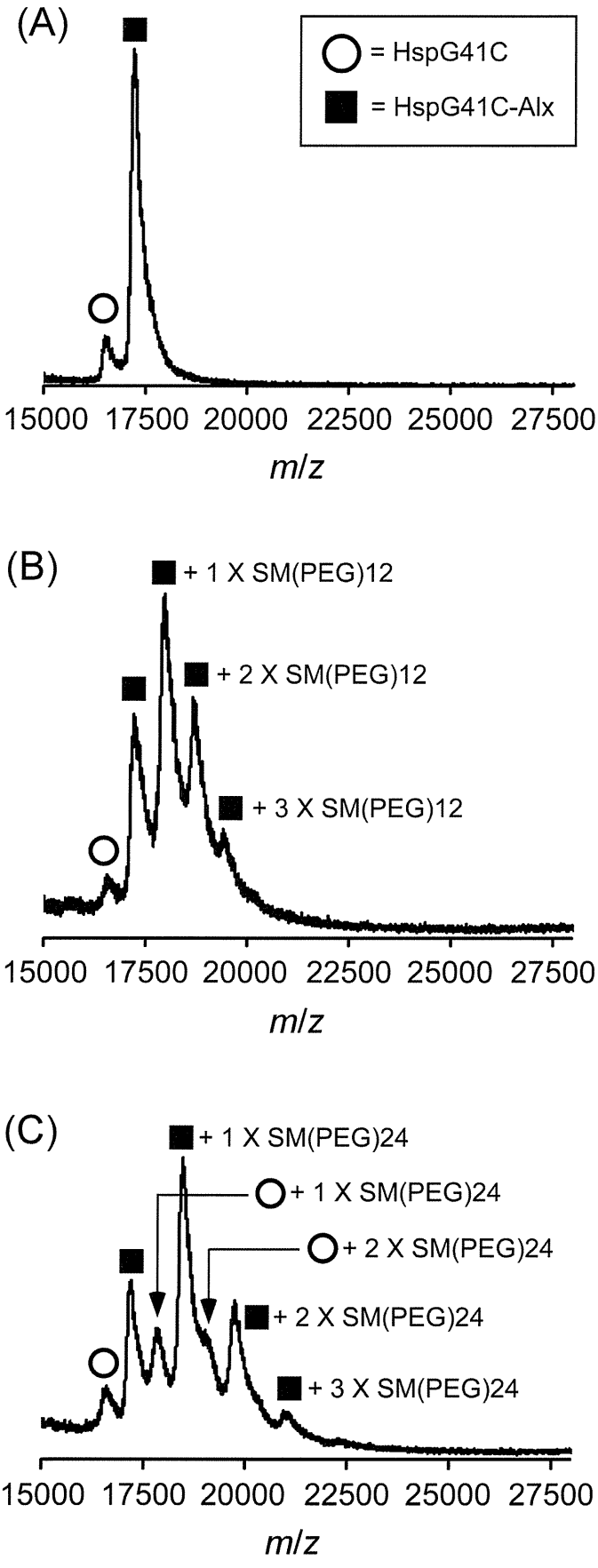
(A)
= HspG41C
= HspG41C-Alx
15000 17500 20000 22500 25000 27500
m/z
(B)
+ 1 X SM(PEG)12
+ 2 X SM(PEG)12
+ 3 X SM(PEG)12
15000 17500 20000 22500 25000 27500
m/z
(C)
+ 1 X SM(PEG)24
+ 1 X SM(PEG)24
+ 2 X SM(PEG)24
+ 2 X SM(PEG)24
+ 3 X SM(PEG)24
15000 17500 20000 22500 25000 27500
m/z

Figure 3.

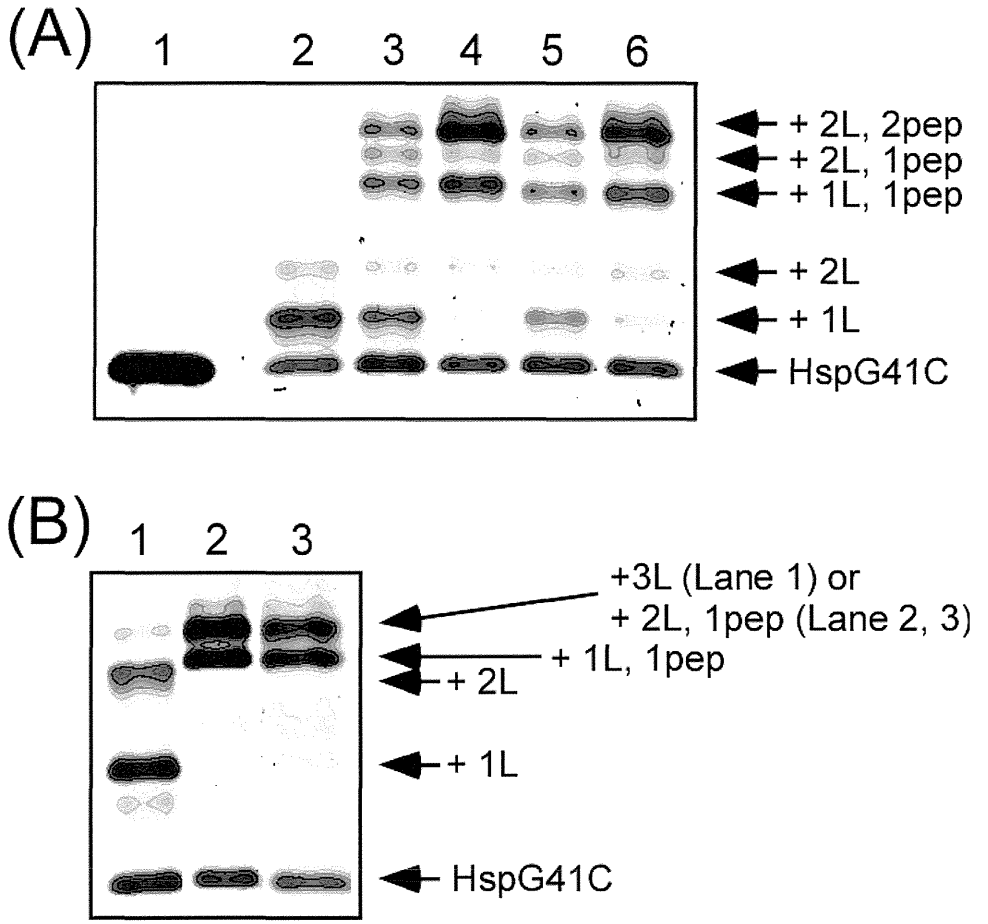
(A)
1
2
3
4
5
6
+ 2L, 2pep
+ 2L, 1pep
+ 1L, 1pep
+ 2L
+ 1L
HspG41C
(B)
1
2
3
+3L (Lane 1) or
+ 2L, 1pep (Lane 2, 3)
+ 1L, 1pep
+ 2L
+ 1L
HspG41C

Figure 4.

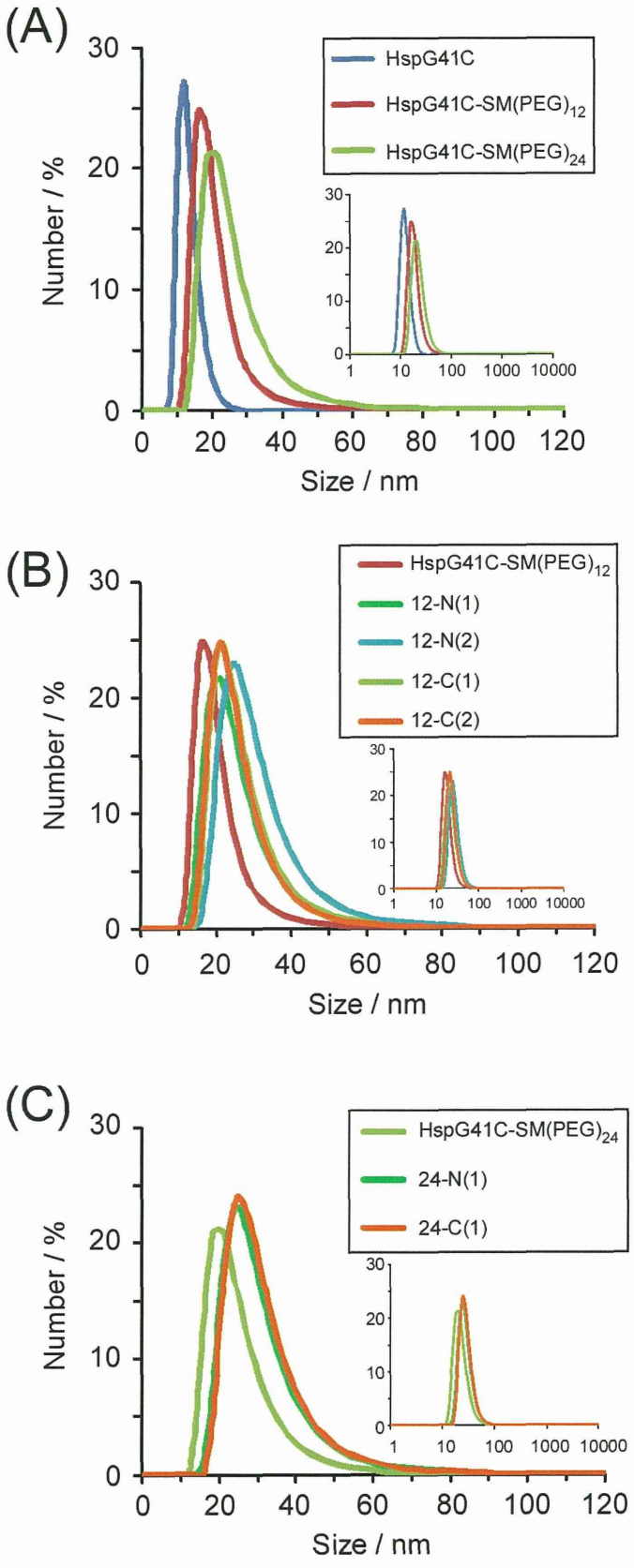
(A)
HspG41C
HspG41C-SM(PEG)12
HspG41C-SM(PEG)24
Number / %
Size / nm
(B)
HspG41C-SM(PEG)12
12-N(1)
12-N(2)
12-C(1)
12-C(2)
Number / %
Size / nm
(C)
HspG41C-SM(PEG)24
24-N(1)
24-C(1)
Number / %
Size / nm

Figure 5.

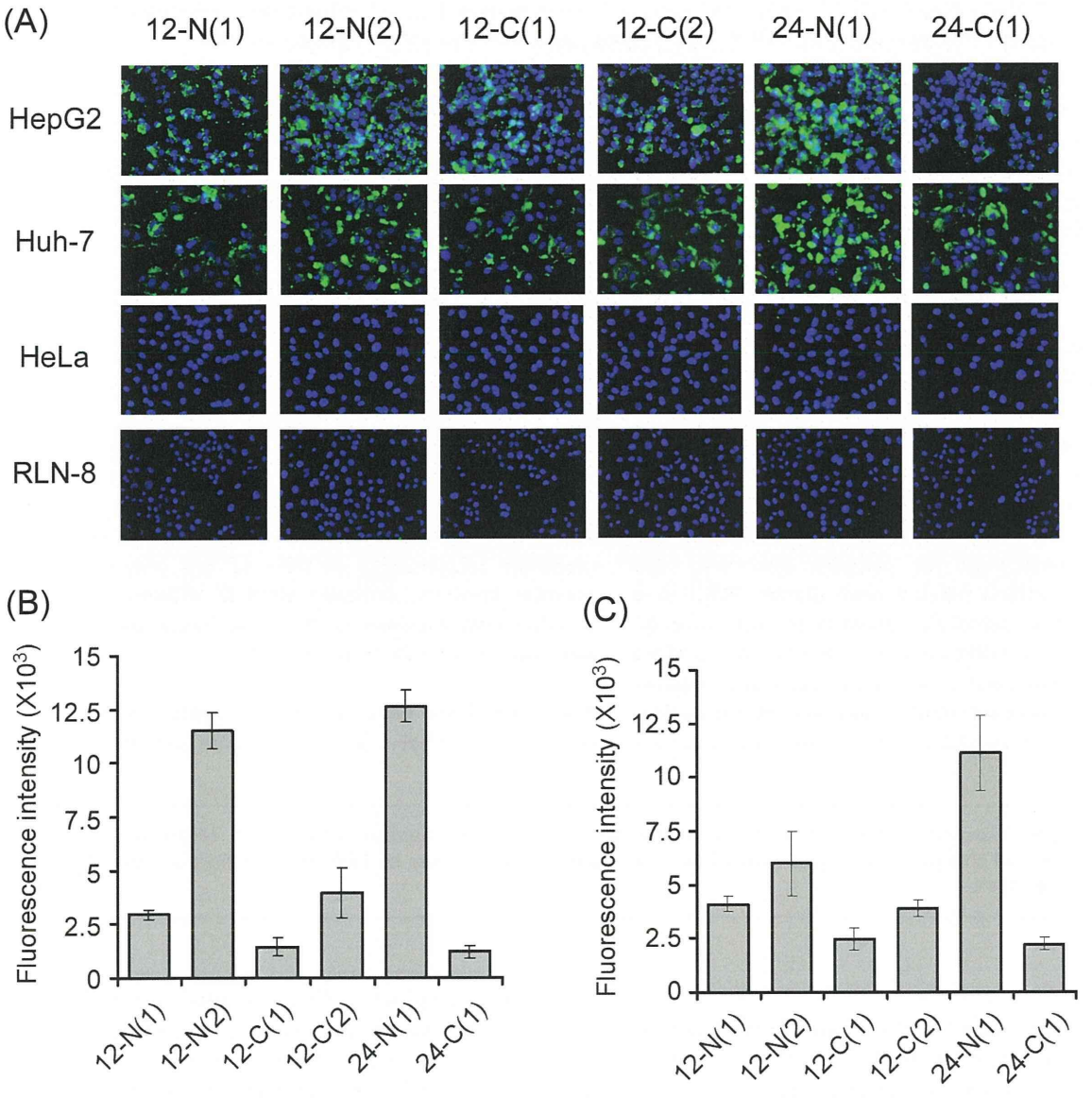
(A)
12-N(1)
12-N(2)
12-C(1)
12-C(2)
24-N(1)
24-C(1)
HepG2
Huh-7
HeLa
RLN-8
(B)
Fluorescence intensity (X10³)
15
12.5
10
7.5
5
2.5
0
12-N(1)
12-N(2)
12-C(1)
12-C(2)
24-N(1)
24-C(1)
(C)
Fluorescence intensity (X10³)
15
12.5
10
7.5
5
2.5
0
12-N(1)
12-N(2)
12-C(1)
12-C(2)
24-N(1)
24-C(1)

Improvement in the colloidal stability of protein kinase-responsive polyplexes by PEG modification

Akira Tsuchiya,[1]* Yuki Naritomi,[1]* Satoshi Kushio,[1] Jeong-Hun Kang,[2] Masaharu Murata,[3,4] Makoto Hashizume,[3,4] Takeshi Mori,[1,5,6] Takuro Niidome,[1,5,6] Yoshiki Katayama[1,4,5,6]

[1]Graduate School of System Life Sciences, Kyushu University, 744 Motooka, Nishi-ku, Fukuoka 819-0395, Japan
[2]Department of Biomedical Engineering, National Cerebral and Cardiovascular Center Research Institute, 5-7-1 Fujishiro-dai, Suita, Osaka 565-8565, Japan
[3]Center for Advanced Medical Innovation, Kyushu University, 3-1-1 Maidashi, Higashi-ku, Fukuoka 812-8582, Japan
[4]International Research Center for Molecular Systems, 744 Motooka, Nishi-ku, Fukuoka 819-0395, Japan
[5]Department of Applied Chemistry, Faculty of Engineering, Kyushu University, 744 Motooka, Nishi-ku, Fukuoka 819-0395, Japan
[6]Center for Future Chemistry, Kyushu University, 744 Motooka, Nishi-ku, Fukuoka 819-0395, Japan

Received 17 October 2011; accepted 29 November 2011
Published online 15 February 2012 in Wiley Online Library (wileyonlinelibrary.com). DOI: 10.1002/jbm.a.34049

Abstract: We have reported a disease-cell specific gene expression system that is responsive to intracellular signaling proteins (e.g., protein kinases and proteases) hyperactivated in diseased cells. For this system, cationic peptide-grafted polymers were synthesized for polyplex formation with genes. Here, we modified poly(ethylene glycol) (PEG) to a protein kinase A (PKA)-responsive polymer to improve polyplex stability. PEG modification neutralized the surface charge of the polyplex and successfully increased polyplex stability at physiological conditions. However, PEG modification (PEG contents, 0.6 and 3.3 mol %) showed almost negligible effects on the reactivity of grafted peptides to PKA and the promotion of gene expression responding to PKA activity. Excessive modification of PEG (PEG contents, 6.8 mol %) inhibited polyplex formation. These results indicate that moderate modification of PEG to the enzyme-responsive polymer improves polyplex stability without inhibiting the reaction with enzymes. © 2012 Wiley Periodicals, Inc. J Biomed Mater Res Part A: 100A: 1136–1141, 2012.

Key Words: gene delivery, protein kinase, polyethylene glycol, signal-responsive polymer, colloidal stability

How to cite this article: Tsuchiya A, Naritomi Y, Kushio S, Kang J-H, Murata M, Hashizume M, Mori T, Niidome T, Katayama Y. 2012. Improvement in the colloidal stability of protein kinase-responsive polyplexes by PEG modification. J Biomed Mater Res Part A 2012:100A:1136–1141.

INTRODUCTION

Gene therapy has been expected to be an efficient method for the treatment of diseases that are difficult to cure (e.g., cancer). To replace viral gene carriers, various synthetic carriers such as cationic polymers, cationic lipids, and peptides have been developed to deliver therapeutic genes to target diseased cells.[1–3] Although the cationic polymers readily form complexes with plasmid DNA (pDNA) via electrostatic interactions, the cationic surface charges of polymer/pDNA complexes (polyplexes) allow nonspecific adsorption of blood components such as serum albumin (SA) in the bloodstream, and genes are eliminated through the reticuloendothelial system before reaching target diseased cells.[4] Degradation of the pDNA of the polyplexes by serum nucleases is also a problem. One of the techniques used to address these issues is polyanion coating onto polyplexes. To coat the polyplexes with polyanions such as chondroitin sulfate and hyaluronic acid has been shown to improve the colloidal stability of the polyplexes and to achieve efficient delivery of genes.[5,6] Another technique is the modification of poly(ethylene glycol) (PEG) to cationic gene carriers.[7–9] PEG is a hydrophilic, neutral polymer. It is widely used as a biomaterial because of unique properties such as nontoxicity, nonimmunogenicity, and reduced nonspecific adsorption of plasma proteins by the excluded volume effect.[10] Hence, PEG-modified gene carriers provide a long blood circulation time to pDNA and accumulate in solid tumors by the enhanced permeation and retention effect.[11,12]

Moreover, delivery of specific genes to targeted diseased cells without adverse effects upon normal cells is needed to increase the safety and efficiency of gene therapy. We recently developed a novel gene-regulation system called

*These authors contributed equally to this work.
Correspondence to: Y. Katayama; e-mail: ykatatcm@mail.cstm.kyushu-u.ac.jp
Contract grant sponsors: Japan Science and Technology Agency, Japanese Ministry of Education, Science, Sports, and Culture (Grant-in-Aid for Scientific Research)

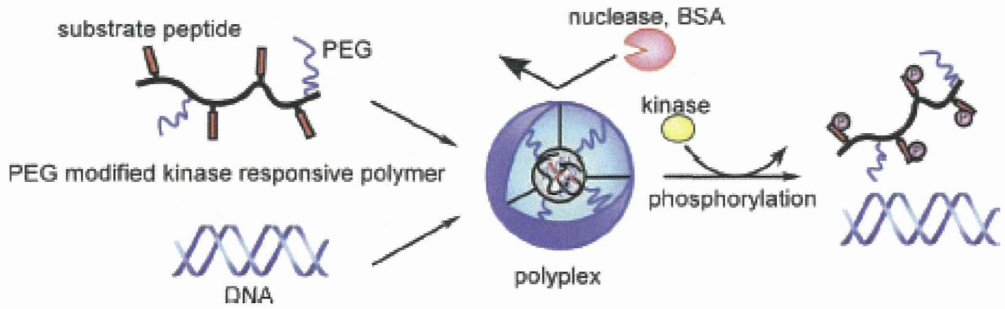

FIGURE 1. Gene regulation system using a PEG-modified kinase-responsive polymer. PEG-modified kinase-responsive polymers formed polyplexes with DNA through electrostatic interactions. The PEG surface layer on the polyplex inhibited nonspecific adsorption of BSA and degradation of pDNA. After transfection, peptide substrates in the polymer were phosphorylated by an activated kinase and gene expression was activated. [Color figure can be viewed in the online issue, which is available at wileyonlinelibrary.com.]

drug or gene delivery system responding to cellular signals (D-RECS) that specifically expresses genes in diseased cells.[13–16] This system utilizes hyperactivation of certain protein kinases to distinguish diseased cells from normal cells. Protein kinases have essential roles in intracellular signal transduction pathways, and hyperactivation of particular protein kinases often causes various diseases (including certain types of cancer).[17,18] For example, cAMP-dependent protein kinase (PKA) and protein kinase C (PKC)α are hyperactivated in many cancers such as colon cancers, melanoma, and breast cancers.[15,19–21] For the D-RECS system, we have synthesized an artificial gene regulator possessing a neutral backbone and cationic peptide side chains that are substrates of targeted protein kinases. The electrostatic interaction between the polymers and pDNA can be modulated by phosphorylation of the peptide substrates due to a decrease in their cationic charges. Thus, transgenes are specifically expressed in diseased cells. We have developed some gene-regulation systems responding to protein kinases such as PKA,[13] PKCα,[14] Rho-kinase,[15] and Iκ-B kinase β.[16]

In the present study, we prepared a new version of a peptide-grafted polymer containing several PEG graft chains to improve the stability of polyplexes. PKA was selected as the target protein kinase (Fig. 1). We clarified an optimal grafting density of the PEG chains satisfying stability in serum conditions and responsive gene expression to protein kinase activity.

EXPERIMENTAL PROCEDURES

Peptide syntheses

The protected peptide substrate of PKA, H-βAla-LR(Pbf)R-(Pbf)AS(tBu)LGW(Boc)-NH_2, was synthesized according to standard 9-fluoroenylmethyloxycarbonyl (Fmoc)-chemistry procedures on 2-chlorotrityl chloride resin. The protected peptide was liberated from the resin by treatment with 1% trifluoroacetic acid (TFA) in dichloromethane and purified by precipitation from water.

Polymer syntheses

The initiator, 2,2′-azobis (2-methylpropionitrile; Wako Pure Chemical Industries, Tokyo, Japan), was added into a solution of *N*-isopropylacrylamide (NIPAM; Wako) and *N*-acryloyloxysuccinimide (NAS; Kokusan Chemical, Tokyo, Japan) in anhydrous *N,N*-dimethyl formamide (DMF; Kanto Chemical, Tokyo, Japan). Polymerization was carried out at 60°C for 18 h under a nitrogen atmosphere. Poly(NIPAM-*co*-NAS) was collected by reprecipitation from diethyl ether and dried *in vacuo*. The molar ratio of each monomeric unit was determined by ^{1}H NMR.

To graft the protected peptide, poly(NIMAP-*co*-NAS) was dissolved in DMF/chloroform (1:1, *v/v*) solution, and the protected peptide was added to the solution. The reaction was carried out at room temperature for 3 days with stirring. Resulting polymers were collected by reprecipitation from diethyl ether and dried *in vacuo*. Polymers were dissolved in DMF/chloroform solution again and amino-terminus PEG (MW = 5000; NOF, Tokyo, Japan) added to the solution to modify PEG onto the polymer. The reaction was carried out at room temperature for 3 days with stirring of the sample. To cap the remaining activated ester groups, a 10-equiv amount of isopropylamine (Wako) was added to the solution, and the resulting mixture was stirred at room temperature for 3 days. Polymers were collected by reprecipitation from diethyl ether and dried *in vacuo*. To remove the protecting groups of the grafted peptide, polymers were treated with 94% TFA (Kanto Chemical) containing 2.5% triisopropylsilane, 2.5% water, and 1.0% 1,2-ethanedithiol (Sigma-Aldrich, St. Louis, MO). After reprecipitation from diethyl ether, resulting polymers were dialyzed for 3 days against water. The contents of the peptide and PEG in the polymers were determined by the UV absorption of tryptophan and elemental analyses.

Dynamic light-scattering measurement of polyplexes

The diameters of the polyplexes were measured using Zetasizer Nanoseries (Malvern Instruments, Worcestershire, UK) at a detection angle of 173° and temperature of 25°C. A residual molar mixing ratio [nitrogen/phosphorus (N/P) ratio] was defined as the ratio of a residual molar concentration of amino groups of arginine units in the polymer to that of phosphate groups in pDNA. Polyplexes were prepared by mixing the polymer with pDNA solution at various N/P ratios in distilled water followed by incubation for 15 min at room temperature. The final concentration of pDNA was adjusted to 2.5 μg/mL by 10 m*M* HEPES buffer (pH = 7.4).

For the evaluation of the stability of the polyplexes in the presence of sodium chloride and bovine serum albumin

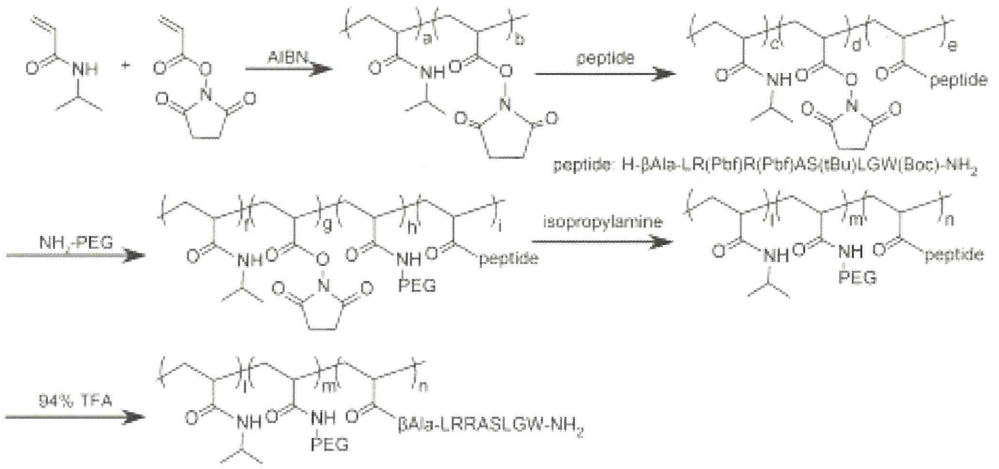

SCHEME 1. Synthetic scheme of NPAK-PEG.

(BSA), we prepared polyplexes at an N/P ratio of 8.0. The final concentration of pDNA was adjusted to 2.5 μg/mL in 10 m*M* phosphate buffer (pH = 7.4) containing 150 m*M* sodium chloride and 50 μg/mL BSA (Sigma-Aldrich). A light scattering count rate of the polyplex solution was then monitored every 5 min for 1 h.

Analyses of the ζ-potential of polyplexes

The ζ-potential of polyplexes was measured using Zetasizer Nanoseries at a scatter angle of 17° and temperature of 25°C. Samples were prepared by the same method as the dynamic light-scattering measurement of polyplexes.

Gel retardation assay

pDNA (0.3 μg) and polymers were incubated at room temperature for 15 min for polyplex formation. Fetal bovine serum (20%) was added into the polyplex and the resulting mixture incubated at 37°C for 1 h. A large excess of poly (sodium 4-styrenesulfonate) (100 equiv to pDNA) was added to the solutions to exclude pDNA from the polymers. The resulting solutions were analyzed by electrophoresis using 1% agarose gel at 100 V for 25 min.

Coupled enzyme assay

Phosphorylation of the grafted peptide in the polyplex was monitored using a coupled enzyme assay. The complex or peptide alone was diluted to 100 μL (final concentration of the peptide, 30 μ*M*) in 10 m*M* HEPES (pH = 7.4) containing 1 m*M* phosphoenolpyruvate (Wako), 10 U/μL lactate dehydrogenase (LDH; Sigma-Aldrich), 4 U/μL pyruvate kinase (Wako), 200 μ*M* adenosine triphosphate (ATP; Sigma-Aldrich), 1 m*M* $MgCl_2$, 300 μ*M* nicotinamide adenine dinucleotide (NADH), and 10 U/μL PKA (Promega, Madison, WI). The reaction was carried out at 25°C of NADH consumption was detected by monitoring absorbance at 340 nm with a UV/Vis spectrometer (UV-2550; Shimadzu, Tokyo, Japan) equipped with an SPR-8 temperature controller (Shimadzu).

Luciferase expression assay using a cell-free system

Cell-free expression experiments were done using a T7 Quick Coupled Transcription/Translation System (Promega). Polyplexes were prepared at various N/P ratios by mixing the polymers with pDNA for 15 min. Final volumes were adjusted to 10 μL by 10 m*M* HEPES buffer (pH = 7.4). Exactly 20 μL of T7 Quick Master Mix and 0.5 μL of 1 m*M* methionine were added to polyplex solutions and incubated at 37°C for 90 min. After reaction completion, 100 μL of luciferin solution was added to 10 μL of the reaction mixture and chemiluminescence measured using a Multilabel Counter (ARVO SX; Wallac, Turku, Finland).

For evaluation of gene expression responding to PKA activity, polyplexes were phosphorylated at 37°C for 2 h in 10 m*M* HEPES buffer (pH = 7.4) containing 1 m*M* $MgCl_2$, 200 μ*M* ATP, and 1 U/μL PKA (total volume, 10 μL). After the phosphorylation reaction, a cell-free gene expression was demonstrated by the same procedures described above. As a negative control, heat-inactivated PKA treated at 97°C for 3 min was used.

RESULTS AND DISCUSSION

Polymer syntheses

We previously synthesized signal-responsive polymers by radical copolymerization between hydrophilic monomers and methacryloyl-modified peptides.[13–15] However, regulating the content of peptides and PEG moieties in the polymer chain using such methods is not easy. In particular, the vinyl monomer possessing PEG units may not be suitable for radical polymerization due to steric hindrance. Therefore, we developed a new synthetic route to modify peptides and PEG units onto the main chain (Scheme 1). First, the polymer main chain was prepared by copolymerization between NIPAM and NAS. The content of the NAS unit in the resulting polymer was determined by ^{1}H NMR to be 9.7 mol %.

Then, the peptide substrate (H-βAla-LR(Pbf)R(Pbf)AS(t-Bu)LGW(Boc)-NH_2) of PKA and amino-terminated PEG (molecular weight (MW = 5000) were modified onto the main chain. We used a peptide substrate in which the side

TABLE I. Contents of Peptides and PEG for Each Polymer

	Peptide Contents		PEG Contents	
Polymer	mol %	wt %	mol %	wt %
NPAK	3.5	26	–	–
NPAK-PEG(0.6)	3.5	21	0.6	17
NPAK-PEG(3.3)	3.5	12	3.3	54
NPAK-PEG(6.8)	3.5	7.8	6.8	71

groups were protected to avoid undesirable reactions. After the modification of peptide and PEG, the remaining active-ester groups were reacted with *N*-isopropylamine. Finally, the protected groups were removed from the grafted peptide. The peptides and PEG contents in the resulting polymers are shown in Table I. We obtained four polymers [NPAK, NPAK-PEG(0.6), NPAK-PEG(3.3), and NPAK-PEG(6.8)] with a constant content of peptide chains and varying content of PEG chains.

Analyses of the ζ-potential of polyplexes

We evaluated the ζ-potentials of polyplexes at an N/P ratio of 8.0 in 10 m*M* HEPES buffer (pH = 7.4). The ζ-potential of the polyplex of NPAK was +13 mV (Fig. 2). This cationic surface charge should be derived from the peptide substrate grafted onto the polymer, which has +2 net charges. For PEG-modified polymers, the ζ-potential of the polyplexes became neutral with an increase in PEG content (Fig. 2). This result reflected successful shielding of the cationic charge of the polyplex by modified PEG chains.

Suppression of gene expression

We evaluated the suppression of gene expression by each polyplex using a cell-free gene expression system driven by T7 RNA polymerase (Fig. 3). NPAK completely suppressed gene expression at N/P ratios of ≥2.0. For PEG-modified polymers, suppression of gene expression weakened with an increase in PEG content. This finding indicated weak condensation of pDNA in the polyplex due to suppression of electrostatic interaction by bulky PEG chains. The weak condensation of pDNA in the polyplex would afford an access of T7 RNA polymerase. Moreover, NAPK-PEG(6.8) possessing the highest density of PEG chain promoted gene expression. The mechanism for this phenomenon is not clear, but similar promotion of gene expression has also been identified from block copolymers between poly(L-lysine) and PEG.[23]

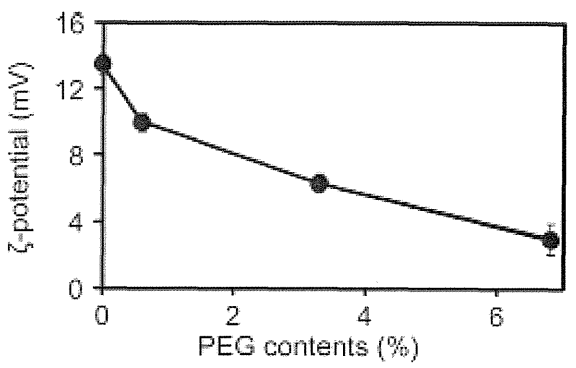

FIGURE 2. Analyses of the ζ-potential of polyplexes at an N/P ratio of 8.0. Data are mean ± SEM for three experiments.

Stability of polyplexes

Polyplexes are usually aggregated in blood due to the shielding of surface charges by high salt concentrations[24] or adsorption of anionic plasma proteins.[25] Aggregation of polyplexes reduces the efficacy of delivery to target diseased cells. In this experiment, we evaluated the stability of NPAK-PEG/pDNA polyplexes in phosphate-buffered saline (PBS) containing 50 μg/mL BSA. Polyplexes were prepared at an N/P ratio of 8.0, and their stability evaluated by changes in diameter and light-scattering count rate. For NPAK, the diameter [Fig. 4(A)] and count rate [Fig. 4(B)] of polyplexes increased drastically on addition of sodium chloride and BSA into samples due to interparticle coagulation. Polyplexes of PEG-modified NPAKs showed a decrease in diameter, indicating suppression of polyplex aggregation by PEG modification. An excluded volume effect of the grafted PEG chains mainly improved the stability of polyplexes, but the polyNIPAM main chain may also contribute to such improved stability because it becomes more dehydrated at physiological temperatures.[26] The hydrophobic nature of polyNIPAM would augment the stability of polyplex *via* hydrophobic interactions.

Interestingly, the count rate of the polyplexes of PEG-modified NPAKs was reduced by the addition of sodium chloride and BSA, showing an increase in the density of these polyplexes. This increase could be ascribed to condensation of the polyplexes through shielding of their excess cationic charge and/or a further dehydration of the PolyNIPAM main chain due to a salting-out effect.

Protection of pDNA degradation

We evaluated if PEG-modified polymers can protect pDNA from degradation by nucleases under the 20% serum condition (Fig. 5). After incubation with serum for 1 h, naked pDNA was completely degraded. When pDNA formed polyplexes with NPAK, NPAK-PEG(0.6), or NPAK-PEG(3.3), pDNA

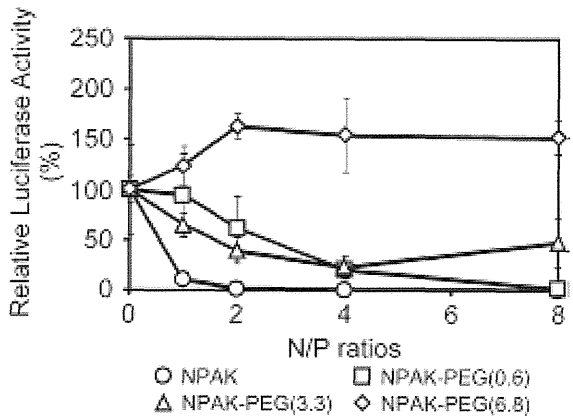

FIGURE 3. Analyses of luciferase expression of polyplexes at each N/P ratio using the cell-free expression system. Relative luminescence units were calculated by normalizing the luminescence for each polyplex to that of free pDNA. Data are mean ± SEM for three experiments.

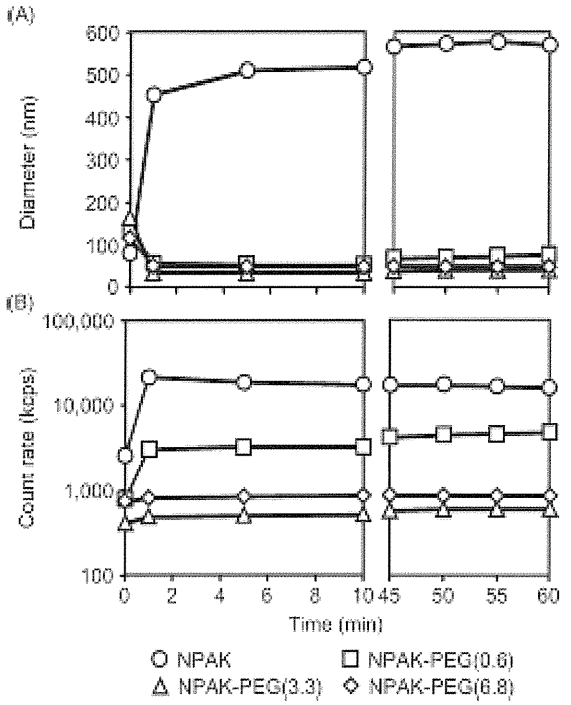

FIGURE 4. Changes in the diameters (A) and light scattering count rates (B) of polyplexes in buffer solution containing 150 m*M* sodium chloride and 50 μg/mL BSA. Polyplexes were prepared by mixing pDNA with NPAK (circle), NPAK-PEG(0.6) (square), NPAK-PEG(3.3) (triangle), or NPAK-PEG(6.8) (diamond) at an N/P ratio of 8.0.

was well protected from this degradation. However, for NPAK-PEG(6.8), pDNA was cleaved by nucleases, and full-length pDNA completely disappeared. These results suggested that the highest content (6.8) of PEG loosened the polyplex and afforded an access of the nucleases to pDNA.

Phosphorylation of polyplexes

To achieve gene regulation responding to cellular protein kinases, the peptide substrates grafted on PEG-modified polymers must be phosphorylated by PKA after forming polyplexes. Thus, we evaluated the influence of PEG modification on the phosphorylation of peptides by PKA using a coupled enzyme assay. In this assay, the phosphorylation of peptide was monitored by the decrease in absorbance at 340 nm derived from consumption of NADH (Fig. 6). The peptides grafted onto each polymer were phosphorylated irrespective of PEG contents. These results showed that PEG

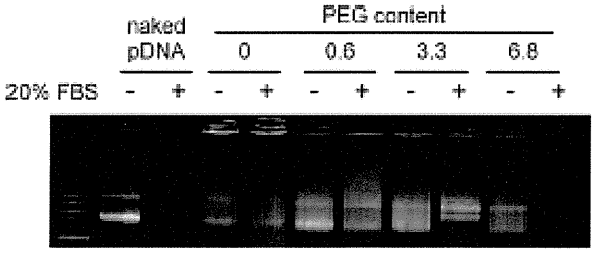

FIGURE 5. Enzymatic degradation of polyplexes. Polyplexes prepared at an N/P ratio of 8.0 were incubated with 20% fetal bovine serum and applied to 1 wt % agarose gel.

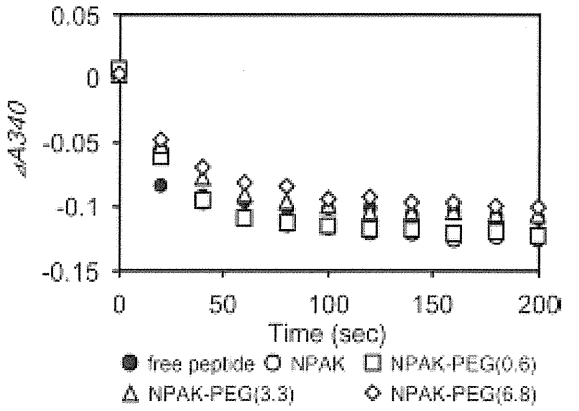

FIGURE 6. Time-dependent monitoring of phosphorylation for peptide alone (closed circle) and polyplexes [NPAK (open circle), NPAK-PEG(0.6) (square), NPAK-PEG(3.3) (triangle), and NPAK-PEG(6.8) (diamond)] by the coupled enzyme assay. Phosphorylation of peptide and polymer was determined by detecting the change in consumption of NADH (ΔA340) in the absorbance at 340 nm.

modification had no effect on the phosphorylation of peptides by PKA.

Gene regulation using NPAK-PEG

We evaluated whether phosphorylation of grafted-peptides by PKA can promote gene expression. We used the three polymers [NPAK, NPAK-PEG(0.6), and NPAK-PEG(3.3)] that showed effective suppression of gene expression as observed in Figure 3. After the phosphorylation reaction of each polyplex, the polyplex was applied to the cell-free gene expression system. When heat-inactivated PKA was used as a negative control, all polymers suppressed gene expression compared with that in the naked pDNA. Addition of activated PKA to each polyplex increased gene expression at NPAK-PEG(0.6) and NPAK-PEG(3.3) (Fig. 7). NPAK suppressed gene expression, but its peptides were phosphorylated by PKA (Fig. 6). The lack of gene expression in NPAK may have been caused by the hydrophobic nature of the polyNIPAM main chain. Because of hydrophobic interactions, the polyplex is not dissociated even after phosphorylation.

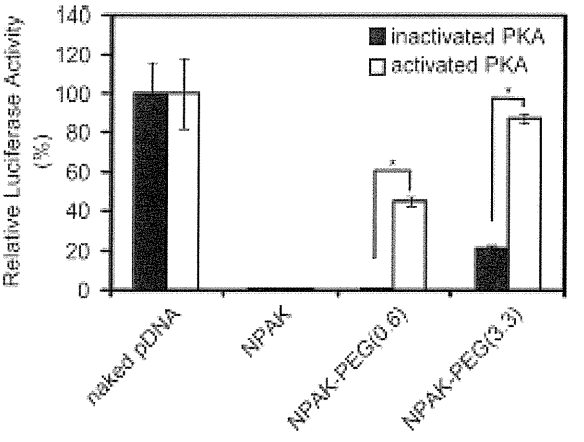

FIGURE 7. PKA-responsive gene expression of polyplexes. Polyplexes were prepared at an N/P ratio of 8.0. Relative luminescence units were calculated by normalizing the luminescence for free pDNA. Data are mean ± SEM for three experiments.*$p < 0.01$.

For PEG-modified polymers, PEG chains loosened the polyplexes, resulting in effective dissociation of the polyplex after phosphorylation and gene expression.

CONCLUSION

We synthesized novel PEG-modified polymers that respond to PKA activation. PEG modification stabilized the polyplex and protected the aggregation induced by sodium chloride and BSA. If the PEG content of polymers was optimized (0.6 and 3.3 mol %), polymers suppressed the attack of nucleases to pDNA but had no effect on the phosphorylation of peptide substrates and gene expression. These results indicate that moderate modification of PEG to enzyme-responsive polymers improve the stability of the polyplex without inhibition of the reaction with enzymes.

REFERENCES

1. Masago K, Itaka K, Nishiyama N, Chung U, Kataoka K. Gene delivery with biocompatible cationic polymer: Pharmacogenomic analysis on cell bioactivity. Biomaterials 2007;28:5169–5175.
2. Radchatawedchakoon W, Watanapokasin R, Krajarng A, Yingyongnarongkul B. Solid phase synthesis of novel asymmetric hydrophilic head cholesterol-based cationic lipids with potential DNA delivery. J Bioorg Med Chem 2010;18:330–342.
3. Powton CW, Lucas P, Thomas BJ, Uduehi AN, Milroy DA, Moss SH. Polycation-DNA complexes for gene delivery: A comparison of the biopharmaceutical properties of cationic polypeptides and cationic lipids. J Control Release 1998;53:289–299.
4. Faraji AH, Wipf P. Nanoparticles in cellular drug delivery. Bioorg Med Chem 2009;17:2950–2962.
5. Jeon O, Yang HS, Lee TJ, Kim BS. Heparin-conjugated polyethyleneimine for gene delivery. J Control Release 2008;132:236–242.
6. Ito T, Iida-Tanaka N, Koyama Y. Efficient in vivo gene transfection by stable DNA/PEI complexes coated by hyaluronic acid. J Drug Target 2008;16:276–281.
7. Takae S, Miyata K, Oba M, Ishii T, Nishiyama N, Itaka K, Yamasaki Y, Koyama H, Kataoka K. PEG-detachable polyplex micelles based on disulfide-linked block catiomers as bioresponsive nonviral gene vectors. J Am Chem Soc 2008;130:6001–6009.
8. Rimann M, Luhmann T, Textor M, Guerino B, Ogier J, Hall H. Characterization of PLL-*g*-PEG-DNA nanoparticles for the delivery of therapeutic DNA. Bioconjug Chem 2008;19:548–557.
9. Merdan T, Kunath K, Petersen H, Bakowsky U, Voigt KH, Kopecek J, Kissel T. PEGylation of poly(ethylene imine) affects stability of complexes with plasmid DNA in a dose-dependent manner after intravenous injection into mice. Bioconjug Chem 2005;16:785–792.
10. Wattendorf U, Merkle HP. PEGylation as a tool for the biomedical engineering of surface modified microparticles. J Pharm Sci 2008;97:1–15.
11. Niidome T, Ohga A, Akiyama Y, Watanabe K, Niidome Y, Mori T, Katayama Y. Controlled release of PEG chain from gold nanorods: Targeted delivery to tumors. Bioorg Med Chem 2010;18:4453–4458.
12. Maeda H. The enhanced permeability and retention (EPR) effect in tumor vasculature: The key role of tumor-selective macromolecular drug targeting. Adv Enzyme Regul 2001;41:189–207.
13. Oishi J, Kawamura K, Kang JH, Kodama K, Sonoda T, Murata M, Niidome T, Katayama Y. An intracellular kinase signal-responsive gene carrier for disordered cell-specific gene therapy. J Control Release 2006;110:431–436.
14. Kang JH, Asai D, Kim JH, Mori T, Toita R, Tomiyama T, Asami Y, Oishi J, Sato YT, Niidome T, Jun B, Nakashima H, Katayama Y. Design of polymeric carriers for cancer-specific gene targeting: Utilization of abnormal protein kinase Cα activation in cancer cells. J Am Chem Soc 2008;130:14906–14907.
15. Tsuchiya A, Kang JH, Asai D, Mori T, Niidome T, Katayama Y. Transgene regulation system responding to Rho associated coiled-coil kinase (ROCK) activation. J Control Release 2011;155:40–46.
16. Asai D, Tsuchiya A, Kang JH., Kawamura K, Oishi J, Mori T, Niidome T, Shoji Y, Nakashima H, Katayama Y. Inflammatory cell-specific transgene expression system responding to Iκ-B kinase beta activation. J Gene Med 2009;11:624–632.
17. Nishizuka Y. The role of protein kinase C in cell surface signal transduction and tumor promotion. Nature 1984;308:693–698.
18. Cohen P. The role of protein phosphorylation in human health and disease. Eur J Biochem 2001;268:5001–5010.
19. Carlson CC, Smithers SL, Yeh KA, Burnham LL, Dransfield DT. Protein kinase A regulatory subunits in colon cancer. Neoplasia 1999;4:373–378.
20. Kenneth WL, Barbara L, Richard MN. Retinoic acid increases cyclic AMP-dependent protein kinase activity in murine melanoma cells. J Biol Chem 1980;255:5999–6002.
21. Gordge PC, Hulme MJ, Clegg RA, Miller WR. Elevation of protein kinase A and protein kinase C activities in malignant as compared with normal human breast tissue. Eur J Cancer A 1996;32:2120–2126.
22. Tomiyama T, Toita R, Kang JH, Asai D, Shiosaki S, Mori T, Niidome T, Katayama Y. Tumor therapy by gene regulation system responding to cellular signal. J Control Release 2010;148:101–105.
23. Osada K, Oshima H, Kobayashi D, Doi M, Enoki M, Yamasaki Y, Kataoka K. Quantized folding of plasmid DNA condensed with block catiomer into characteristic rod structures promoting transgene efficacy. J Am Chem Soc 2010;132:12343–12348.
24. Ko YT, Kale A, Hartner WC, Sternberg BP, Torchilin VP. Self-assembling micelle-like nanoparticles based on phospholipid-polyethyleneimine conjugates for systemic gene delivery. J Control Release 2009;133:132–138.
25. Lin S, Wang Y, Ji S, Liang D, Yu L, Li Z. An acid-labile block copolymer of PDMAEMA and PEG as potential carrier for intelligent gene delivery system. Biomacromolecules 2008;9:109–115.
26. Ganta S, Devalapally H, Shahiwala A, Amiji M. A review of stimuli-responsive nanocarriers for drug and gene delivery. J Control Release 2008;126:187–204.

Cite this: *Chem. Commun.*, 2011, **47**, 12388–12390

www.rsc.org/chemcomm

COMMUNICATION

Electrochemical signal modulation in homogeneous solutions using the formation of an inclusion complex between ferrocene and β-cyclodextrin on a DNA scaffold†

Toshihiro Ihara,*[ab] Tsugutoshi Wasano,[a] Ryuta Nakatake,[a] Pelin Arslan,[a] Akika Futamura[a] and Akinori Jyo[a]

Received 29th August 2011, Accepted 9th October 2011
DOI: 10.1039/c1cc15365j

Two DNA conjugates modified with ferrocene and β-cyclodextrin were prepared as a pair of probes that work cooperatively for DNA sensing, in which the electrochemical signal of ferrocene on one probe was significantly "quenched" by the formation of an inclusion complex with β-cyclodextrin of the other probe on the DNA templates.

Various analytical platforms based on electrochemical responses have been proposed for studying specific interactions involving nucleic acids and/or proteins.[1,2] Most of these methods, however, require one of the participants in the interactions to be immobilized on the electrode because signal contrasts arise as the result of changes in the distance between the electrochemically active probe and the electrode surface on the targeted events (= change in the local concentration of the probe on the electrode). Generally, the preparation of biomolecule-modified electrodes is time-consuming and it is difficult to obtain reproducible results. We have already reported some electrochemical methods for DNA analysis.[3] In this series of studies, a gene sensor was developed based on the interactions between a ferrocene (Fc)-modified DNA probe and a DNA-modified electrode.[4] Fluorimetry for DNA sensing using β-cyclodextrin (βCyD)-modified DNA has also recently been reported.[5,6] It is known that βCyD binds tightly with Fc to form an inclusion complex, and the electrochemical activity of Fc accommodated in the βCyD cavity is suppressed by being shielded from the bulk solution.[7] βCyD could therefore be regarded as a "quencher" for electrochemical signals, similar to an azo-quencher for FRET-based fluorimetry.[8] This means that specific interactions could be monitored using the electrochemical signals of Fc in homogeneous solutions, if the inclusion complex is formed quantitatively in accordance with the relevant interactions. This would free the preparation of electrochemical molecular sensors from the need to anchor the molecules on the electrodes.[9]

Here we examined the possibility of electrochemical signal modulation in a homogeneous solution using the controlled interaction between two DNA conjugates carrying Fc and βCyD on one end of synthetic oligodeoxyribonucleotides (ODN). All the ODNs used in this study are shown in Fig. 1. The sequences of the two conjugates (**Fc-ODN$_n$** and **CyD-ODN$_n$**) were designed to be complementary to the adjacent sites of the targets (**target27** and **target22N**: a part of the TPMT gene[10]). A pair of the two conjugates forms a tandem duplex with the target, in which both modified units are directed convergently and, hopefully, form a quenched inclusion complex at the center of the duplexes. This could be regarded as a split probe (or binary probe) in electrochemistry.[11]

The system of tandem duplex 1 was subjected to UV melting experiments to examine the interactions between βCyD and Fc on the DNA framework. All the curves showed biphasic features with two inflection temperatures caused by successive meltings (T_{max}).‡[12] The meltings at lower and higher temperatures are

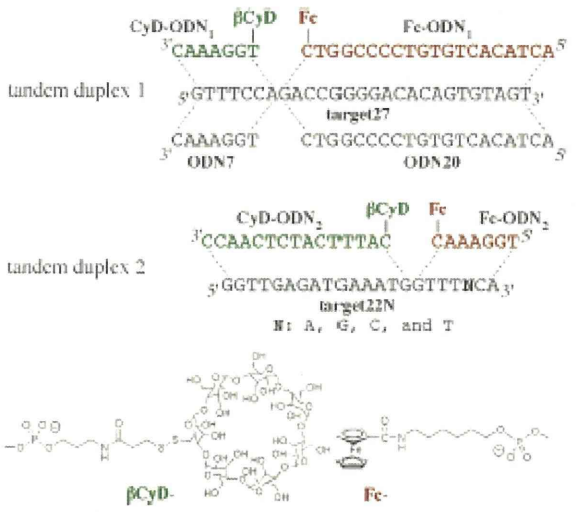

Fig. 1 Sequences of synthetic oligodeoxyribonucleic acids used in this study. Two tandem duplexes (1 and 2) were designed. They consist of **CyD-ODN**, **Fc-ODN**, and the targets (a part of the TPMT gene). **ODN7** and **ODN20** are the unmodified ODNs as references.

[a] *Department of Applied Chemistry and Biochemistry, Kumamoto University, 2-39-1 Kurokami, Kumamoto 860-8555, Japan. E-mail: toshi@chem.kumamoto-u.ac.jp; Tel: +81 96 372-3772*
[b] *CREST, JST, Tokyo 102-0075, Japan*

† Electronic supplementary information (ESI) available: ODN conjugates synthesis and results of UV melting, SWVs, and hydrodynamic voltammograms. See DOI: 10.1039/c1cc15365j